



Practice article

A new fault feature extraction method of rolling bearings based on the improved self-selection ICEEMDAN-permutation entropy

Maohua Xiao^{a,*}, Zhenyu Wang^a, Yuanfang Zhao^a, Guosheng Geng^a, Schahram Dustdar^b, Praveen Kumar Donta^b, Guojun Ji^c

^a College of Engineering, Nanjing Agricultural University, Nanjing 210031, China

^b Distributed Systems Group, TU Wien, Vienna, 1040, Austria

^c Essen Agricultural Machinery Changzhou Co., Ltd., Changzhou 213000, China

ARTICLE INFO

Keywords:

Rolling bearings
Feature extraction
ICEEMDAN
Permutation entropy

ABSTRACT

The vibration signals of rolling bearings are complex and changeable, and extracting meaningful features is difficult. Currently, the commonly used empirical mode decomposition (EMD) algorithms have the problem of mode aliasing. In this paper, a new feature extraction method based on the improved complete ensemble empirical mode decomposition with adapted noise (ICEEMDAN) and permutation entropy is proposed. In this method, the ICEEMDAN algorithm is first improved and optimized to enable a self-selection function. The vibration signal is then decomposed into several intrinsic modal functions using this algorithm, and the permutation entropy is extracted as the fault feature of rolling bearings, which improves the accuracy of fault classification and realizes the intelligent feature extraction of different fault states. Then, the Case Western Reserve University dataset is used for verification, and the results show that this scheme can effectively separate the vibration signal characteristics of bearings in different states, and can be used to characterize the characteristics of different bearing signals. Finally, based on the mechanical transmission system bearing experimental platform independently developed by our school, the experimental results show that compared with the unimproved ICEEMDAN algorithm, the diagnostic accuracy rate of the proposed method is 99.5%, which is increased by 6.4%, and it can be effectively used for feature extraction of rolling bearings.

1. Introduction

Rolling bearings are widely used in rotating machinery [1]. Given the advantages of its high precision, low cost and long service life, it is widely used in wind power generation, shipbuilding, aerospace and other fields [2]. However, about 50% of motor failures in mechanical equipment are caused by damage to rolling bearings [3]. Therefore, the fault diagnosis of rolling bearings has always been a hot and difficult point in the study of the stable operation of mechanical equipment. When a bearing fails, its vibration signal contains a large amount of fault characteristic information, showing nonlinear, non-stationary and intermittent characteristics [4]. For this type of fault diagnosis, it is helpful to improve the diagnosis efficiency and accuracy [5,6]. The process of mechanical fault diagnosis is essentially a process of fault pattern recognition. Different fault diagnosis methods and pattern recognition methods may have different classification accuracy [7].

Many experts and scholars have studied the fault diagnosis of rolling

bearings. The use of signal processing, neural network, pattern recognition and other methods has continuously improved the efficiency and accuracy of fault diagnosis [8]. Signal processing methods mainly include wavelet de-noising, Fourier transform and modal decomposition [9,10]. The wavelet denoising method is simple and clear, and the calculation speed is fast. However, the scope of application is not very wide, and the denoising effect of white noise widely existing in practical applications is poor. Fourier transform is fast, but it may cause some errors when dealing with unsteady signals, resulting in spectrum aliasing, spectrum leakage and fence effect. However, the signal processing method of modal decomposition avoids data redundancy to some extent, and has a good advantage in processing non-intermittent component signals. With the continuous emergence of new modern processing methods of vibration signals, nonlinear and unsteady time-frequency analysis and other methods are more and more widely used [11], which can effectively extract fault features and improve the diagnosis level of bearing faults. Neural network processing methods include convolution neural network and support vector machine [12,13], which

* Corresponding author.

E-mail address: xiaomaohua@njau.edu.cn (M. Xiao).

<https://doi.org/10.1016/j.isatra.2023.09.009>

Received 4 August 2022; Received in revised form 12 September 2023; Accepted 13 September 2023

Available online 19 September 2023

0019-0578/© 2023 ISA. Published by Elsevier Ltd. All rights reserved.

Notations used in this paper*Nomenclature*

$x(t)$	Original signal
h_1	The first deviation
m_1	The first average of the sum of the upper and lower envelopes
h_{1k}	Average of the k th upper and lower envelope sums
r_1	The first residual
c_1	The first IMF component
c_i	The i th IMF component
r_n	The n th residual
n	Order of IMF
N	The length of time
k	The number of intrinsic mode function
K	Order of matrix
$x^{(i)}$	New signal after adding noise signal
$D_1(w^{(i)})$	The first noise signal

$D_k(\cdot)$	The k th noise signal
$A(\cdot)$	The operator of local mean
t	Time period
$w^{(i)}$	The i th white noise added
$\beta_0, \beta_1, \dots, \beta_{k-1}$	Adjustment coefficient of the 0th, 1th, ..., $k-1$ th time
X	Time series matrix
Y	Matrix composed of time sequence X
j_1, j_2, \dots, j_m	Column index
$m!$	Number of arrangement modes
m	Phase dimension
P	Probability of the reconstructed component
H_{pe}	Permutation entropy
$w(t)$	Gaussian white noise
$Y(t)$	Composed of four signals
$y_1(t)$	Simulation signal 1
$y_2(t)$	Simulation signal 2
$y_3(t)$	Simulation signal 3

are mainly used for pattern recognition of fault types, thus improving the classification accuracy of signals. Other methods include deep fault feature extraction analysis [14], permutation entropy [15], CNN [16] and so on. With the continuous development of machine learning and big data technology, deep mining of data features has become the future development trend, so signal representation has become the direction of further research.

Empirical mode decomposition (EMD) algorithm is an adaptive signal processing method proposed by Huang et al. [17]. This method decomposes the signal according to its own time scale characteristics, and obtains a limited number of intrinsic mode functions (IMF) [18]. Each IMF component contains local characteristic signals of the original signal with different time scales. Compared with traditional signal processing methods, this method is intuitive, direct, posterior and adaptive [19]. However, there are still some phenomena of endpoint extension and modal aliasing [20,21].

The advantage of EMD algorithm is that it can better reflect the physical characteristics of vibration signals, but it also has some limitations. When dealing with vibration signals with intermittent components, it is easy to produce modal aliasing, which leads to the wrong decomposition results. To solve the modal aliasing problem of EMD, many experts and scholars have proposed further improved algorithms (e.g., ensemble empirical mode decomposition (EEMD) [22–24], complementary ensemble empirical mode decomposition (CEEMD) [25–27], complete ensemble empirical mode decomposition with adaptive noise (CEEMDAN) [28–30], and so on) and verified their anti-noise.

Among these algorithms, CEEMDAN has the best signal decomposition effect, but some problems (e.g., slow-running speed and a large amount of calculation) also exist. The reason is that it needs to add complex noise signals to the original signal, and it does not fundamentally solve the problem of modal aliasing. Therefore, experts and scholars further put forward the algorithm of improved complete ensemble empirical mode decomposition with adapted noise (ICEEMDAN) [31], which can reduce the reconstruction error of the intrinsic mode function (IMF) and is widely used in traffic, earthquake, fault diagnosis, and other fields. Special noise is added to the signal processing process for the ICEEMDAN algorithm, which reduces the residual noise in the IMF component and alleviates the modal aliasing to some extent. However, the addition of special noise also brings some problems, e.g., a large amount of calculation and slow iteration speed. In addition, the selection of key parameters of ICEEMDAN has great influence on the elimination of modal aliasing and noise [32,33]. Therefore, this paper will make an improvement on the basis of ICEEMDAN algorithm. For the intermittent signals in the original signal, ICEEMDAN

algorithm is used for decomposition, while the signals without intermittent signals are decomposed by EMD algorithm, so as to improve the accuracy of adaptive signal feature extraction and speed up iteration.

The permutation entropy algorithm is a signal mutation detection method based on the characteristics of time series, which can effectively amplify the weak changes of time series [34]. It has the following advantages: Simple calculation and strong anti-noise ability; High sensitivity to time and high resolution; The output result is intuitive and has good recognition [35]. Therefore, it has a good effect when applied to fault signal feature extraction of rolling bearings.

The commonly used EMD algorithms have a problem with modal aliasing, and removing the noise is difficult and decomposing takes a long time because of the addition of complex noise. To solve the aforementioned problems and accurately extract the features of the rolling bearing's running state, this paper proposes a new feature extraction for the rolling bearings vibration signal based on an improved self-selected ICEEMDAN and permutation entropy algorithm. Improving the ICEEMDAN algorithm adaptively decomposes the vibration signal of rolling bearings and obtains the intrinsic mode function, and then extracts the permutation entropy from the intrinsic mode function to characterize the fault characteristics of rolling bearings. Finally, the experiment was carried out on the bearing experimental platform of mechanical transmission system, and compared with EMD, EEMD, ICEEMDAN and other algorithms. The results show that the self-selected ICEEMDAN algorithm has more advantages, and its diagnostic accuracy rate is 99.5%, which is 6.4% higher than that before optimization. It can be effectively used for feature extraction of rolling bearings.

The remaining sections of the paper is organized as follows: Section 2 discuss about the proposed improved self-selection ICEEMDAN-Permutation entropy method. Section 3, we perform the simulation signal test using the existing and proposed approaches. Section 4 test the measured signal. Section 5, we carry out experimental research and analyze the results. Finally, the paper is concluded in Section 6.

2. The proposed improved self-selection ICEEMDAN-Permutation entropy method

2.1. The improved self-selected ICEEMDAN algorithm

2.1.1. Empirical Mode Decomposition (EMD)

Empirical Mode Decomposition (EMD) algorithm is an adaptive analysis method for analyzing nonlinear and nonstationary signal sequences, with a high signal-to-noise ratio [36]. The key to this method is that the complex signal can be decomposed into a finite number of IMF

and a trend component. Each IMF component contains local characteristic signals of different time scales and has the characteristics of self-adaptation. The EMD decomposition process [37] is as follows:

(1) The first step is to determine the local maxima and minima of the signal $x(t)$ to be measured, and use the fitting method to make the upper and lower envelope values of the signal image. Then, the deviation h_1 of the signal to be measured from the average value m_1 will be calculated according to the average value of the upper and lower envelopes.

(2) If h_1 meets the conditions of IMF, it is recorded as the first IMF component of $x(t)$; If h_1 does not meet the conditions of IMF, the above steps will be repeated k times, so that h_{1k} will meet the conditions of IMF, and the first IMF component obtained through the above steps will be marked as c_1 .

(3) Then, the difference between the signal $x(t)$ and c_1 is taken as the residual r_1 .

$$r_1 = x(t) - c_1 \tag{1}$$

(4) The residual r_1 is used as the original signal, and the above steps are repeated until r_n can no longer decompose the IMF. And finally, n IMF components are obtained.

$$x(t) = \sum_{i=1}^n c_i + r_n \tag{2}$$

From the principle of EMD algorithm decomposition, it can be found that if there is a discontinuous signal in the original signal (a high-frequency signal with a small amplitude appears at a certain moment or a small time interval), the obtained IMF is meaningless.

2.1.2. ICEEMDAN

The ICEEMDAN method is further proposed to solve the problems of CEEMDAN, e.g., slow running speed and mode aliasing. The characteristic of its vibration signal feature extraction is that a special noise is added when extracting the k th IMF. In detail, ICEEMDAN first adds the special noise of non-Gaussian white noise to the decomposition layer of each signal and then decomposes the added special noise signal into a plurality of intrinsic mode functions and corresponding residual signals [38], thus solving the problem of inconsistent IMF numbers.

(1) First, the first noise signal $D_1(w^{(i)})$ is added to the original signal $x(t)$.

$$x^{(i)} = x(t) + \beta_0 D_1(w^{(i)}) \tag{3}$$

where $w^{(i)}$ represents the i th white noise added.

(2) Then, EMD algorithm is used to calculate the local mean value of signal $x^{(i)}$, and the first residual r_1 is obtained by taking the mean value, and the first natural modal function value c_1 is then obtained.

Assuming that the operator of local mean is $A(\cdot)$, the value of the k th intrinsic mode function obtained by EMD decomposition is $D_k(\cdot)$.

$$D_1(x(t)) = x(t) - A(x(t)) \tag{4}$$

$$c_1 = x(t) - r_1 \tag{5}$$

$$c_1 = \frac{1}{I} \sum_{i=1}^I D_I(x(t)) = x(t) - \frac{1}{I} \sum_{i=1}^I A(x^{(i)}) \tag{6}$$

$$r_1 = \frac{1}{I} \sum_{i=1}^I A(x^{(i)}) \tag{7}$$

where I is the number of modal decomposition.

(3) Then, by analogy, noise is added to the $k-1$ residual to get the k

residual, and finally the k intrinsic mode function value will be obtained.

$$c_k = r_{k-1} - r_k \tag{8}$$

$$r_k = \frac{1}{I} \sum_{i=1}^I A(r_{k-1} + \beta_{k-1} D_k(w^{(i)})) \tag{9}$$

According to the comparison, the advantage of ICEEMDAN algorithm used for fault diagnosis signal processing is that it can accurately generate the numerical value of IMF, and can extract features through Fourier spectrum or time domain diagram or directly serve as fault features of rolling bearings.

2.1.3. The improved self-selected ICEEMDAN algorithm

EMD, EEMD, CEEMDAN, and other algorithms encounter some problems when decomposing high-frequency intermittent component signals, e.g., a large calculation error and slow iteration speed. Among them, the high-frequency intermittent component refers to the weak signal embedded in the signal. The signal component that should belong to one frequency band is mistakenly divided into the signal component of another frequency band, which is the phenomenon of modal aliasing, because of the existence of the high-frequency intermittent component. In the bearing fault diagnosis, the mode aliasing phenomenon will lead to the fault features hidden in the signal being concealed or the wrong features being obtained, thus reducing the diagnosis accuracy.

Based on this, this paper proposes an improved self-selected ICEEMDAN algorithm. In this method, the original signal is accurately decomposed. Firstly, whether an intermittent signal in the signal is detected, the segments with an intermittent signal are decomposed by the ICEEMDAN algorithm, and the segments without an intermittent signal are decomposed by the EMD algorithm to improve the accuracy of adaptive signal feature extraction and further diagnose the bearing fault. Through different signal decomposition methods, the accuracy of indirect signal processing is improved. This method can judge the existence of intermittent signals, so that the signal decomposition mode can be selected adaptively, and the fault features can be extracted effectively.

In this method, whether the high-frequency component in the signal is intermittent or not is judged by the change in the distance between the extreme points of the first IMF [39]. If the distance between the two poles exceeds the set threshold, it is considered that there is a high-frequency component, and the first IMF component contains more signal characteristics. Because the first-order IMF decomposed by the EMD algorithm represents the high-frequency component of the signal, its extreme point corresponds to the extreme point of the original signal in the time sequence. The interval between extreme points of high-frequency signals is small, so the position of intermittent components can be judged by using the interval between extreme points of the first IMF.

The distance between the extreme points suddenly changes at the beginning and end of the intermittent signal because the frequency of the intermittent signal usually processed is higher than the frequency of the background signal in this period. Based on this, the extreme point sequence of the intermittent signal is determined, and then the start and end time of the intermittent signal is predicted by mode or mean prediction [40].

Therefore, the decomposition steps of the improved self-selected ICEEMDAN algorithm are as follows:

Step 1: Check whether an intermittent component exists in the original time series. If there is, follow step 2. Otherwise, follow step 3.

Step 2: Detect the interval of intermittent components by mean value prediction, adding special white noise to the original signal in this interval by using the ICEEMDAN method, and decompose the whole original signal using the EMD algorithm to obtain n IMF and a residual signal.

Step 3: Decompose the original signal by EMD algorithm to obtain n

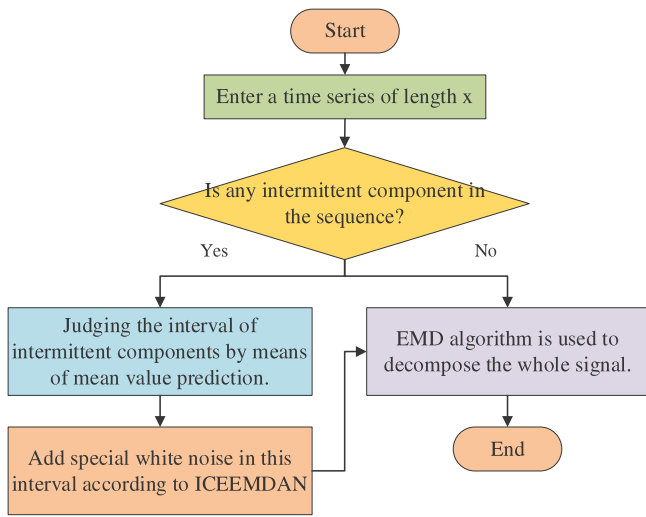


Fig. 1. The flowchart of the improved self-selected ICEEMDAN algorithm steps.

IMF and a residual signal.

The steps to improve the self-selected ICEEMDAN algorithm are shown in Fig. 1. After getting n IMF and a residual signal, it is difficult to distinguish different signals from the waveform, so it is necessary to use the method of quantitative evaluation signal sequence to characterize the signals, and finally input them into the classifier to classify the faults.

2.2. Permutation Entropy (PE)

Permutation entropy is a method that can detect signal mutation and random time series as well as quantitatively evaluate the complexity contained in signal series. The permutation entropy is widely used in fault signal processing because of its strong anti-noise ability, high calculation efficiency and sensitivity to signal mutation. The specific steps are as follows:

(1) Reconstruction of information space

Because the fault signal of rolling bearings is periodic, m groups of data with the same delay time t can be extracted, thus forming the signal space matrix. Through the analysis of space matrix, it is more conducive to the identification of fault types. The reconstructed object is a set of time series X of length N . Then the constructed signal space matrix Y is as follows:

$$Y = \begin{bmatrix} x(1) & x(1+t) & \cdots & x(1+(m-1)t) \\ x(2) & x(2+t) & \cdots & x(2+(m-1)t) \\ x(j) & x(j+t) & \cdots & x(j+(m-1)t) \\ \vdots & \vdots & \ddots & \vdots \\ x(K) & x(K+t) & \cdots & x(K+(m-1)t) \end{bmatrix} \quad (10)$$

$K = N - (m - 1)t$. Each row in matrix Y represents a reconstructed component, and k reconstructed components are noted.

(2) Ascending order

The time period of adjacent data in the signal space matrix Y is t . In order to reflect the arrangement of elements, they need to be arranged in ascending order.

$$\{x(i + (j_1 - 1)t) \leq x(i + (j_2 - 1)t) \leq \cdots \leq x(i + (j_m - 1)t)\} \quad (11)$$

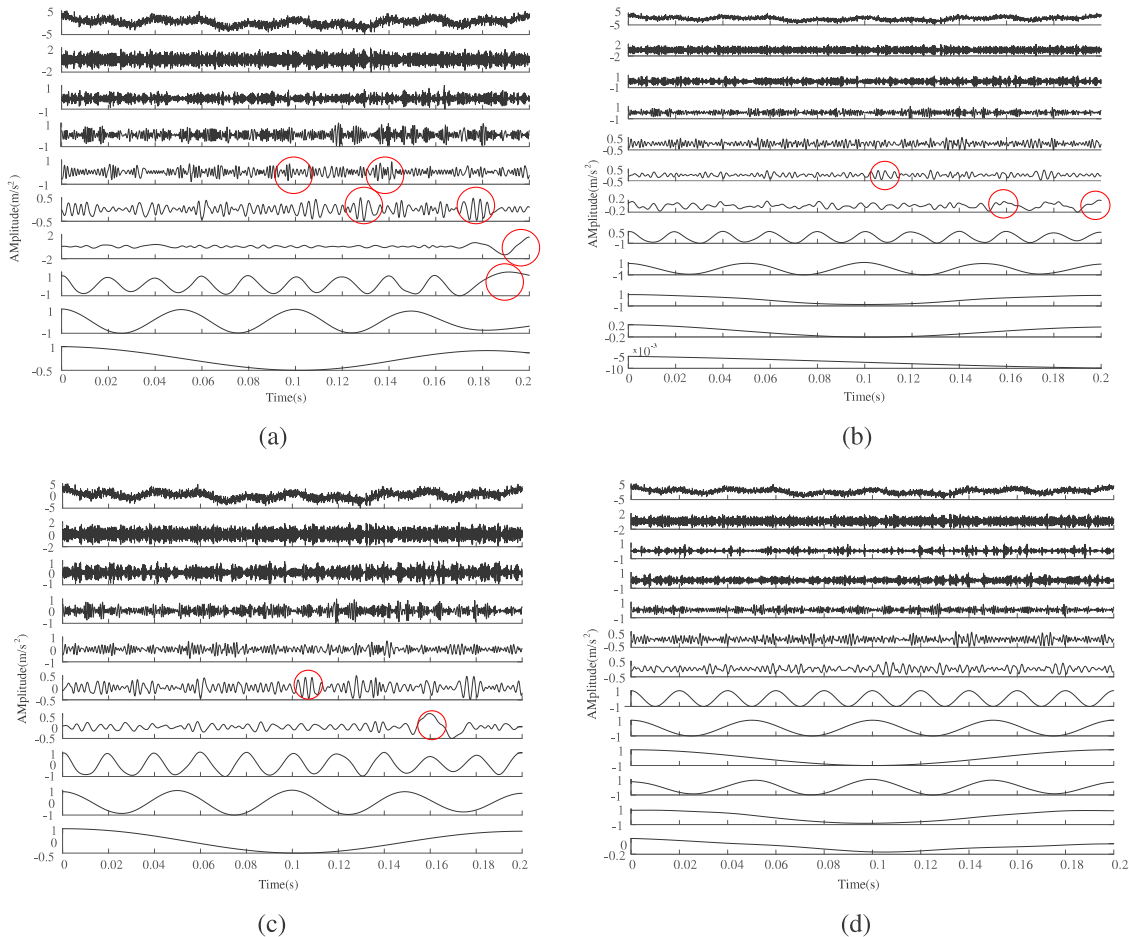


Fig. 2. Time domain diagram is decomposed by four algorithms: (a) time domain diagram of EMD decomposition; (b) time domain diagram of EEMD decomposition; (c) time domain diagram of ICEEMDAN decomposition; and (d) time domain diagram of the improved self-selection ICEEMDAN decomposition.

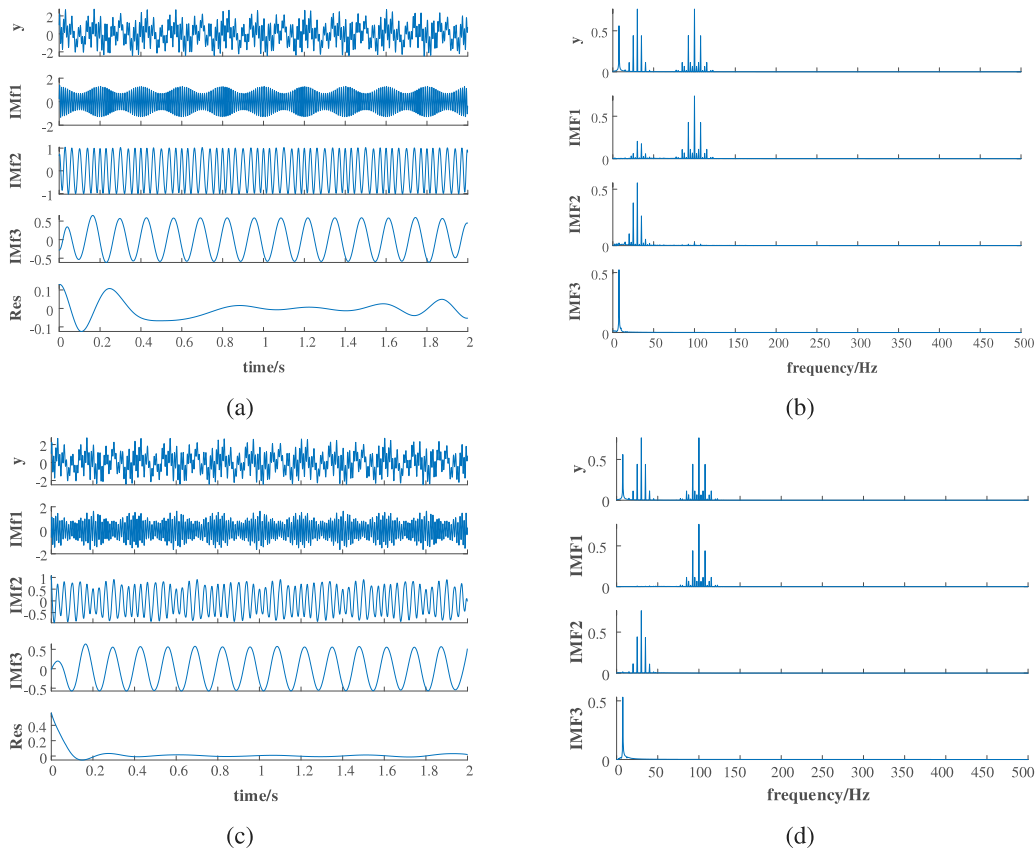


Fig. 3. Modal signal and spectrogram.: (a) Modal signal of ICEEMDAN; (b) Spectrum diagram of ICEEMDAN; (c) Modal signal of the improved self-selection ICEEMDAN; and (d) Spectrum diagram of the improved self-selection ICEEMDAN.

If the elements in the components are equal, the index sequence is obtained by index sorting according to the column in which the elements are located.

$$\{j_1, j_2, \dots, j_m\} \tag{12}$$

By analogy, the index sequence of each reconstructed component will be obtained.

(3) Calculate permutation entropy

The calculated permutation entropy can be used to identify fault signals. When the matrix dimension is m , there are m kinds of arrangement modes of index sequences, and the probability of each sequence is P_r ($r = 1, 2, \dots, N$, $N \leq m!$). The formula for calculating the permutation entropy of time series X is as follows:

$$H_{pe} = - \sum_{r=1}^N P_r \ln P_r \tag{13}$$

The selection of embedding dimension m has great influence on the reconstruction of spatial matrix. If the value of m is too small to reflect the sequence mutation, the ability of the algorithm to detect signal mutation will also be reduced. If the value of m is too large, the length of the reconstructed component will be greatly increased, the sequence will be homogenized, and it is difficult to reflect the slight changes of the sequence, and the amount of calculation will be greatly increased. In the process of practical application, the recommended range of m is [3,7]. Based on experience and research analysis, the embedding dimension m selected in this paper is 5.

(4) Data normalization

For the convenience of use, it is necessary to normalize the permutation entropy. When $P_r = 1/m!$, H_{pe} will reach the maximum value, so the normalized expression is as follows:

$$PE = \frac{H_{pe}}{\ln(m!)} \tag{14}$$

3. Simulation signal test

To verify the superiority of the rolling bearing feature extraction method based on the improved self-selected ICEEMDAN-PE, this section uses EMD, CEEMD, ICEEMDAN and the improved self-selected ICEEMDAN algorithm to decompose the following analog signals.

$$\begin{cases} y_1(t) = \cos(10\pi t) \\ y_2(t) = \cos(40\pi t) \\ y_3(t) = \cos(100\pi t) \\ Y(t) = y_1(t) + y_2(t) + y_3(t) + w(t) \end{cases} \tag{15}$$

where $y_1(t)$, $y_2(t)$, and $y_3(t)$ are the three component signals that make up the analog signal with a sampling frequency of 16 kHz. The added interval of $y_1(t)$ and $y_2(t)$ signals is [0,16000], and the added interval of $y_3(t)$ is [7000,9000], which is used as high-frequency intermittent components. $w(t)$ is Gaussian white noise with a mean value and a variance of 0 and 0.1, respectively. Therefore, $Y(t)$ is composed of four signals.

As shown in Fig. 2, the mixed analog signal is decomposed by EMD, EEMD, ICEEMDAN and the improved self-selected ICEEMDAN algorithm respectively, and different numbers of intrinsic modal functions (IMF) are obtained. It can be seen from each time domain diagram and frequency spectrum diagram that although the number of IMF obtained by EMD algorithm is the smallest, the 4th and 5th IMF after decomposition have strong modal aliasing and distortion at both ends of the signal. Compared with EMD algorithm, the modal aliasing of EEMD and ICEEMDAN algorithm is much reduced, but not completely eliminated, while the modal aliasing of the improved self-selected ICEEMDAN

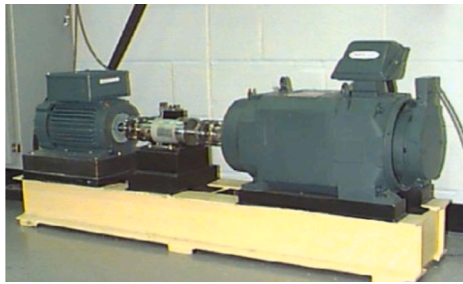


Fig. 4. Bearing fault test bench of Case Western Reserve University.

algorithm is basically eliminated, with high signal integrity and no distortion, and its comprehensive performance is better than other algorithms. In this section, the simulation signals are decomposed by various algorithms, and the advantages of the improved self-selected ICEEMDAN algorithm are verified by visual comparison from the graph. The following section will verify the measured signals through authoritative data sets.

In order to verify the advantages of the algorithm proposed in this paper, a set of simulation signals are constructed for verification. It is mainly composed of three groups of signals x_1 , x_2 and x_3 , in which the

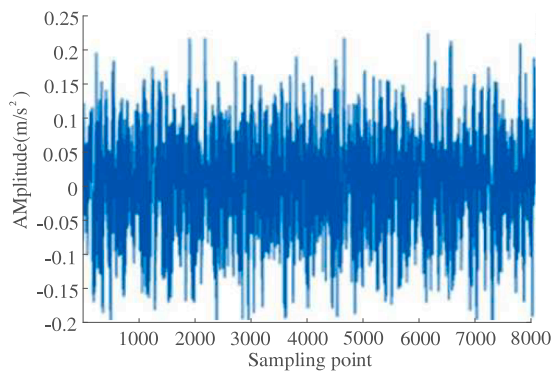
frequency modulation of x_1 signal is 5 Hz and 100 Hz, and the fundamental frequency is 7.5 Hz. The frequency modulation of x_2 is 30 Hz, and the fundamental frequency is 5 Hz. The fundamental frequency of x_3 is 7.5 Hz and 0.1 Hz. The sampling frequency is set at 1000 Hz, the number of sampling points is 2000, and the sampling time is 2 s. The original simulation signal is obtained by superimposing three different signals. Then, the time domain signal of each component signal is converted into frequency domain signal, and its frequency spectrum is drawn. The respective decomposition results are shown in Figs. 3 and 4.

$$\begin{cases} x_1 = (1 + 0.3\cos 10\pi t) \times \sin(200\pi t + \sin 15\pi t) \\ x_2 = \cos(60\pi t + \sin 10\pi t) \\ x_3 = 0.6\sin(15\pi t + 0.2\pi t) \\ y = x_1 + x_2 + x_3 \end{cases} \quad (16)$$

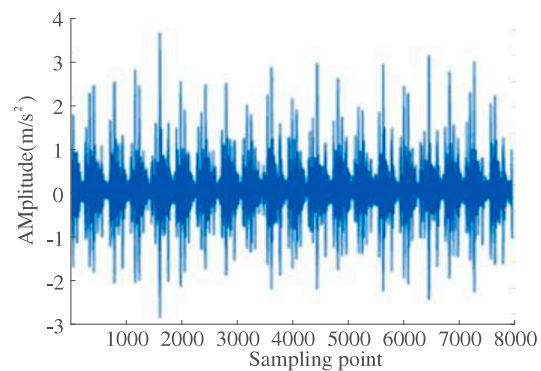
As can be seen from the above figure, the improved self-selected ICEEMDAN can decompose the original simulation signal accurately, and can decompose the original signal according to a specific frequency, resulting in a more stable waveform and less aliasing signals. It can be seen from the IMF1 spectra of the two algorithms that the IMF1 component of ICEEMDAN algorithm has an extra frequency spectrum of 0.2 Hz, which has a certain influence on signal decomposition. However, the improved self-selected ICEEMDAN has less components, less time and more advantages for signal decomposition.

Table 1
Bearing specifications and parameters.

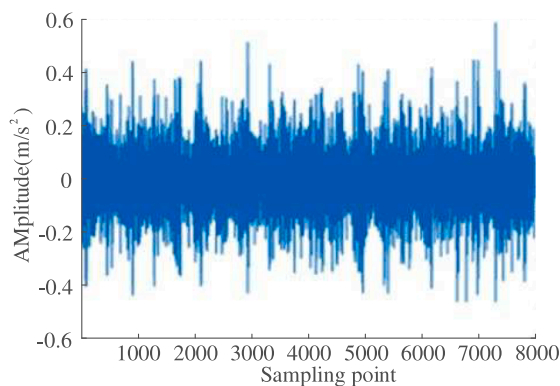
Type	Specifications	Outside diameter/ mm	Inner diameter/ mm	Thickness/ mm	Roller number	Roller diameter/ mm	Nodal diameter/ mm	Contact angle/°
Deep groove ball bearing	6205-2RS	52	25	15	9	7.94	39	0



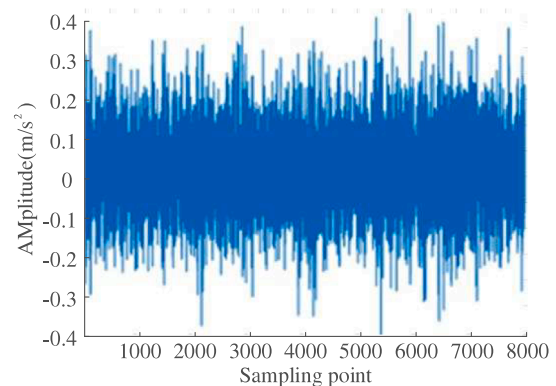
(a)



(b)



(c)



(d)

Fig. 5. Vibration signals of rolling bearings in four different states: (a) normal bearing; (b) inner ring fault bearing; (c) rolling element fault bearing; and (d) outer ring fault bearing.

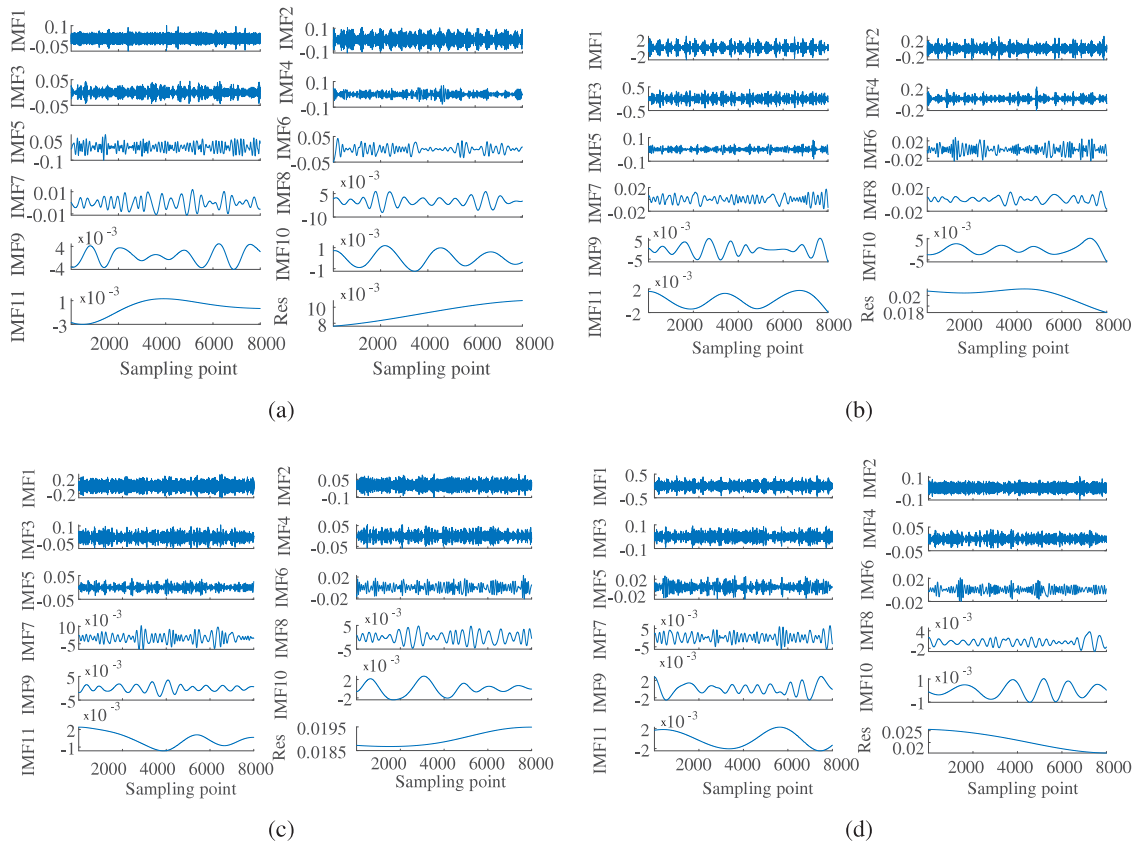


Fig. 6. Vibration signals of rolling bearings in four different states after decomposition: (a) decomposition of normal bearings; (b) decomposition of inner ring fault bearing; (c) decomposition of rolling body fault bearing; and (d) disassembly of outer ring fault bearing.

4. Test of measured signal

In this section, The Case Western Reserve University dataset commonly used in rolling bearing fault diagnosis is used to verify the new feature extraction of the improved self-selected ICEEMDAN and permutation entropy algorithm proposed in this chapter. The bearing failure test bench used by Case Western Reserve University is shown in Fig. 4. The test-bed is equipped with sensor measuring points near the bearings to record data. There are four types of bearings, namely normal bearing, inner ring fault bearing, outer ring fault bearing and rolling element fault bearing. Because this data set is widely used and authoritative in the field of bearing fault diagnosis, this section uses this data set to verify the practicability of the method proposed in this paper.

Select the bearing fault data measured under the condition that the inner ring speed of the bearing is 1797 r/min and the size of the fault point is 0.1778 mm as the research object. Table 1 shows the parameters of the bearing used in the test. Select 8000 sampling points from various bearings, as shown in Fig. 5.

It can be seen from Fig. 4 that the vibration signals of the four states of bearings are quite different, mainly because the vibration signals generated by different faults are different, so their time domain waveforms are also different, which can be used for later analysis. The above four signals are decomposed by the improved self-selected ICEEMDAN to obtain multiple IMF and residual signals, as shown in Fig. 6.

It can be seen from Fig. 6 that 11 IMF components and one residual component are obtained by using the improved self-selected ICEEMDAN decomposition method to decompose the signal. Because it is a time-domain waveform diagram, the fault characteristics can only be judged from the waveform of the curve, which will result in a large error. Because the original signal is complex, with multiple decomposition, there will be the accumulation of errors and other reasons. Therefore, it is necessary to combine these waveform characteristics with the

permutation entropy, and then compare them in the next step by calculating the entropy values. Draw the calculated permutation entropy into a histogram, as shown in Fig. 7.

As can be seen from Fig. 7, there are obvious differences in the arrangement entropy of the bearings. The highest alignment entropy in the normal state is less than that of the faulty bearing. Moreover, the difference of the arrangement entropy of the outer ring fault bearing is relatively obvious, but the arrangement entropy of the inner ring fault bearing and the rolling element fault bearing is similar. In order to facilitate the comparison of different signals, the calculated arrangement entropy value is plotted as a curve for comparison, as shown in Fig. 8.

As can be seen from Fig. 8, although the permutation entropy of each IMF component is concentrated in the normal motion state of the bearing, the entropy value of the normal bearing is smaller than that of the other three kinds of bearing signals with different faults. This is because the energy fluctuation of the vibration signal of the bearing is small, the distribution is uniform and the uncertainty is small. When the bearing is cracked and other faults occur, the energy of the vibration signal changes, which increases the permutation entropy. From the perspective of classification, the permutation entropy of different types of bearing signals is obviously different. Although data coincidence occurs in the later stage of the curve, it does not affect the difficulty of fault data classification. Because the higher data coincidence is mainly the later modal component, and with the increase of decomposition times, the later component has little influence on the fault classification effect, which can be ignored. Through comparison, it can be concluded that the entropy obtained by the improved self-selected ICEEMDAN and permutation entropy algorithm can effectively separate the vibration signal characteristics of bearings in different states, and can be used to characterize the characteristics of different bearing signals.

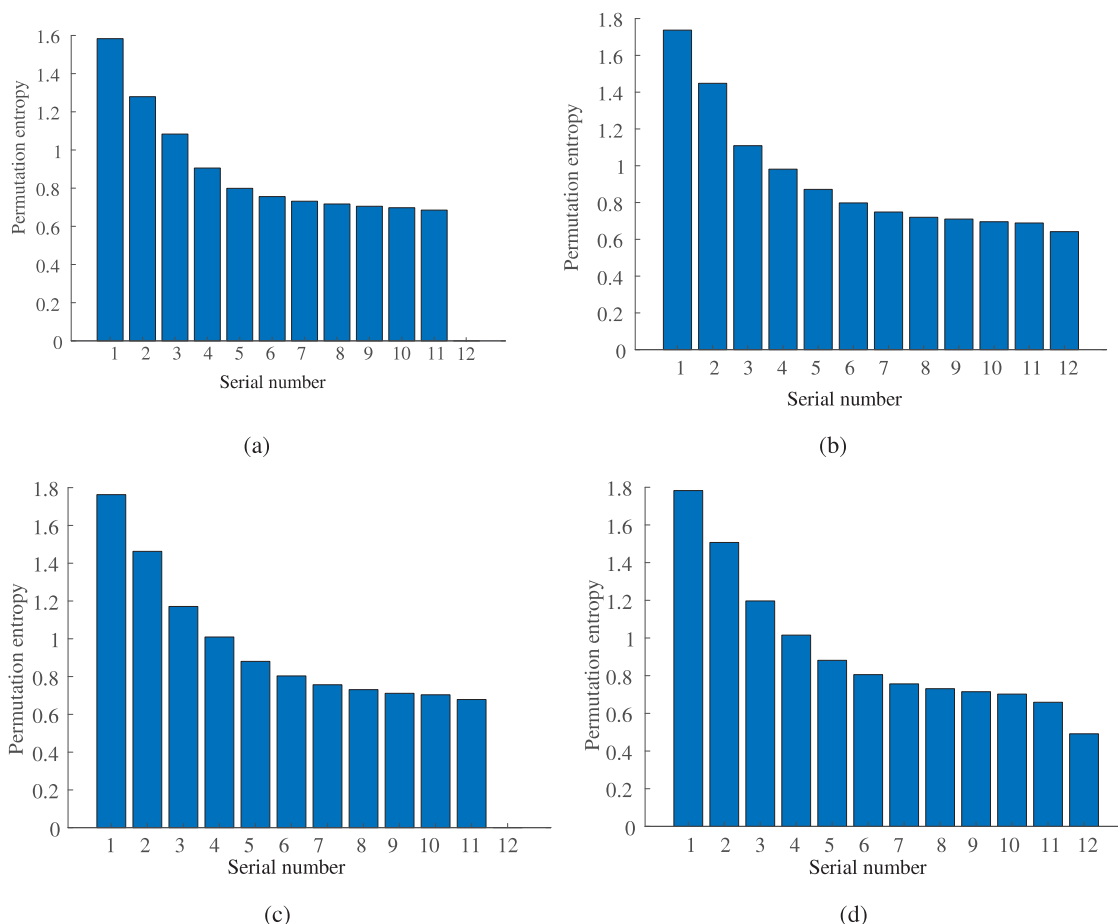


Fig. 7. Four permutation entropy characteristic parameter values: (a) permutation entropy of normal bearing; (b) permutation entropy of inner ring fault bearing; (c) permutation entropy of rolling element fault bearing; and (d) permutation entropy of outer ring fault bearing.

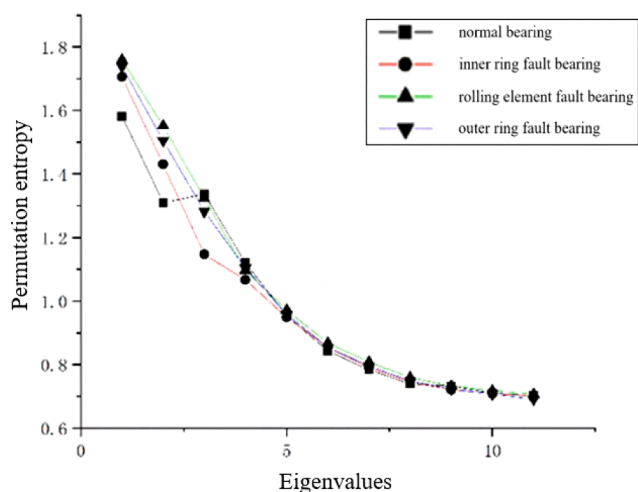


Fig. 8. Permutation entropy line chart of four kinds of bearings.

5. Experimental study

5.1. Scheme design

In order to further verify the effectiveness of the proposed method under actual working conditions, a bench test was carried out. This experiment adopts the mechanical transmission system bearing

experimental platform independently developed by Nanjing Agricultural University, as shown in Fig. 9. The testbed is mainly composed of controller, variable frequency drive motor, bearing seat, coupling, vibration sensor, axial loading device and radial loading device. The controller is responsible for starting the gantry and loading device, and can also accurately adjust the rotating speed. The variable frequency drive motor is mainly responsible for providing power for the motion of the gantry. Sensors are responsible for collecting information. Axial loading device and radial loading device are mainly responsible for adding load to the working bearing to simulate the actual working environment of the bearing and accelerate the damage process of the bearing.

In order to obtain the vibration signal of the rolling bearings in the test bed during operation, signal acquisition equipment is needed. This test is mainly completed by acceleration signal sensor and signal acquisition equipment, as shown in Fig. 10. The model of acceleration sensor is PCB35A26, and its sensitivity is 10.08 mV/g. The signal acquisition device is a 16-channel dynamic information acquisition module. Start the switch of the controller, and adjust the speed of the variable frequency drive motor to 1500 r/min, so that the whole rack can run. The acceleration sensor with a magnet at the bottom is adsorbed on the periphery of the bearing seat of the rolling bearings to be tested. At last, the vibration signal can be transmitted to ZSDASP, the data acquisition and analysis software of the upper computer, through the acquisition equipment, to complete the acquisition and storage. The signal acquisition interface is shown in Fig. 11. One end of the information collector is connected with the acceleration sensor, and the other end needs to be connected with the data acquisition and analysis software on the computer. Set the IP address and connect them successfully.

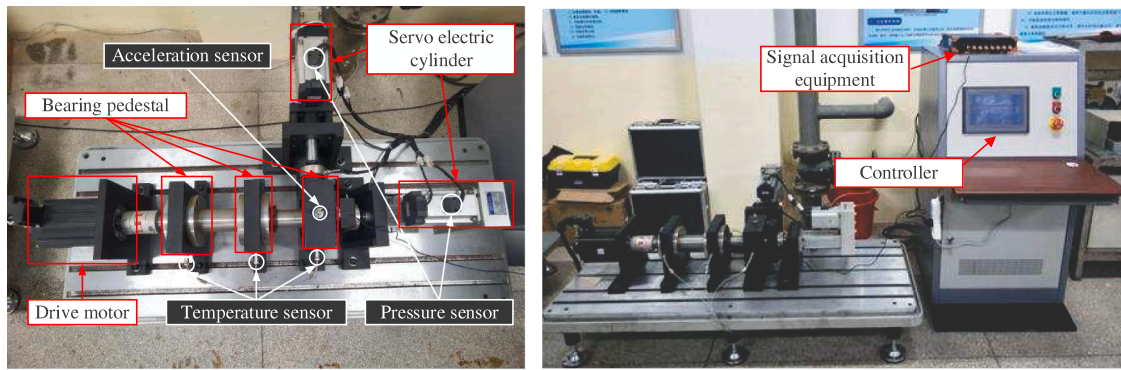


Fig. 9. Bearing experimental platform of mechanical transmission system.



Fig. 10. Schematic diagram of acceleration sensor and signal acquisition card: (a) acceleration sensor; (b) signal acquisition card.

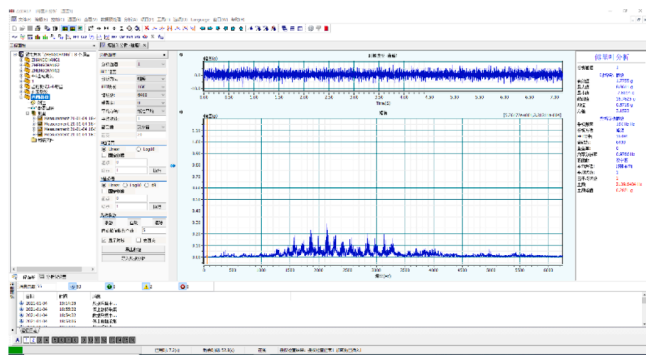


Fig. 11. Signal acquisition interface.

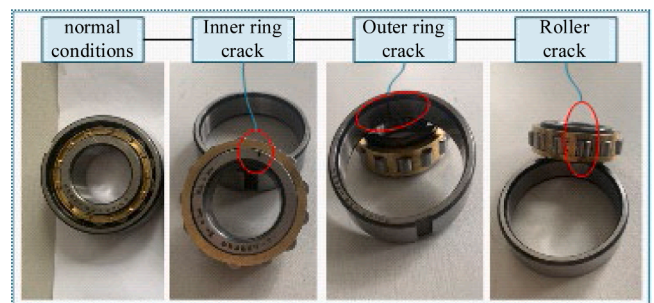


Fig. 12. Four rolling bearings to be tested.

First, create a new acquisition scheme, close all channels 3 to 16, and then fill in the sensitivity parameters of the sensor in channels 1 and 2. The measured physical quantity is changed to acceleration, and various parameters of the analyzer are set, including sampling frequency, sampling mode, duration, etc.

The bearings used in the experiment are cylindrical roller bearings, and the specific parameters are shown in Table 2. In this experiment, a crack with a width of 0.2 mm and a depth of 0.5 mm was processed by laser to simulate the faulty bearing. The actual working condition is simulated by replacing the bearings with different fault types on the bearing seat. Collect the vibration signals of bearings in four states: normal bearing, inner ring fault bearing, outer ring fault bearing and rolling element fault bearing. In order to quantitatively analyze the influence of the new feature extraction method proposed in this paper on the fault diagnosis effect, the common ICEEMDAN algorithm and the improved self-selected ICEEMDAN algorithm proposed in this paper are used for signal decomposition, and then the new feature extraction is carried out by permutation entropy algorithm (see Fig. 12).

5.2. Test procedure

(1) Start the mechanical transmission system equipment bearing experimental platform and ZSDASP acquisition system and collect the bearing vibration signals of normal bearing, inner ring fault bearing, outer ring fault bearing, and rolling element fault bearing. The typical vibration signals of four different states are shown in Fig. 13.

(2) The improved self-selected ICEEMDAN algorithm is used to decompose different fault signals of bearings. The permutation entropy extracted by IMF components after decomposition is used as a feature vector, and a plurality of feature vectors form a feature matrix, which is used as the input of PSO-SVM model. The reliability of the new feature extraction algorithm proposed in this paper is verified by fault diagnosis results.

(3) Too many eigenvalues will affect the training speed, so only the first 8 permutation entropy values of each group of signals are calculated, and an eigenvector is formed. A total of 480 eigenvectors are constructed into a 480-row eigenvector matrix. Due to the large amount

Table 2
Rolling bearings specifications and parameters.

Type	Specifications	Outside diameter/ mm	Inner diameter/ mm	Thickness/ mm	Roller number	Roller diameter/ mm	Nodal diameter/ mm	Contact angle/°
Cylindrical roller bearing	N205EM	52	25	15	13	6.5	38.5	0

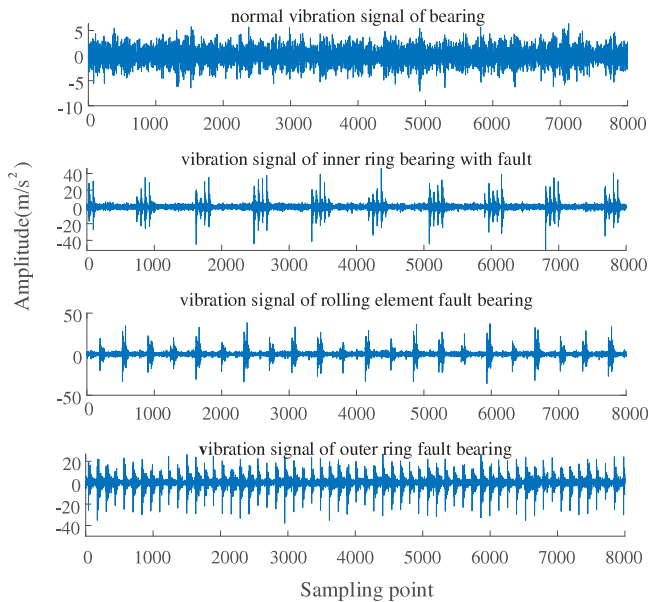


Fig. 13. Vibration signals of rolling bearings in four different states.

of data in the characteristic matrix, Table 3 only lists five characteristic vectors for each bearing type, and uses numbers as labels for different types.

(4) Finally, the characteristic matrix is divided into training samples and testing samples at the ratio of 5 to 1, with the number of 400 and 80 respectively, and each type of bearing is evenly divided, that is, each type of bearing contains 100 groups of training samples and 20 groups of testing samples. The final diagnosis result is shown in Fig. 14.

Fig. 14 shows that the improved self-selected ICEEMDAN algorithm decomposes the vibration signal of rolling bearings, extracts the

permutation entropy features, and uses the SVM improved by PSO for diagnosis, which has excellent results. All the groups of data tested are correctly diagnosed. It shows that this algorithm has a good advantage in feature extraction. To highlight the superiority of the improved self-selected ICEEMDAN algorithm in feature extraction, the decomposition algorithm in the above step (2) is replaced by the common ICEEMDAN algorithm, and the other steps remain unchanged. The diagnosis effect is shown in Fig. 15.

Fig. 15 shows that tags 3 and 4 (which represent the outer ring fault and the rolling element fault, respectively) are confused. This is because the white noise added to the original vibration signal has residue or the noise in the collected signal leads to the mode aliasing phenomenon,

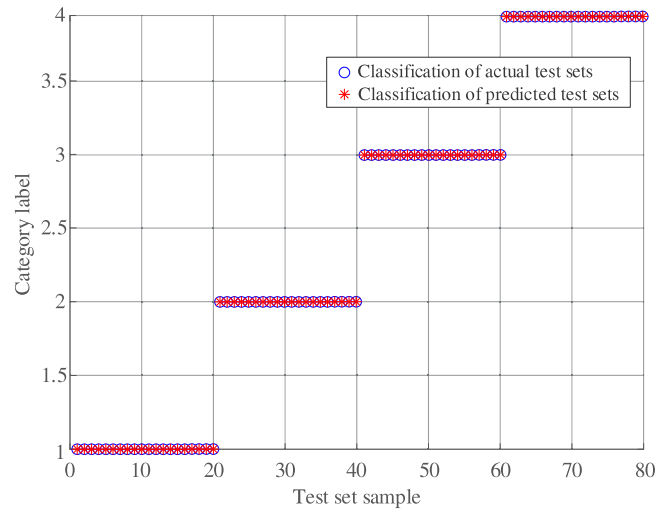


Fig. 14. The diagnosis results obtained by using the improved self-selected ICEEMDAN algorithm.

Table 3
Partial feature vector.

Bearing category	Feature vector									Label
Normal conditions	1.7805	1.5562	1.2803	1.0708	0.9235	0.832	0.7734	0.7386	1	
	1.7831	1.5702	1.2898	1.0824	0.9412	0.8441	0.7752	0.7371	1	
	1.7823	1.5649	1.2806	1.0707	0.9269	0.8347	0.7752	0.7362	1	
	1.7828	1.5683	1.2756	1.0693	0.9397	0.8387	0.7712	0.7440	1	
	1.7831	1.5644	1.2858	1.0730	0.9272	0.8229	0.7634	0.7353	1	
Inner ring fault	1.7454	1.5256	1.2582	1.0697	0.9195	0.8312	0.7837	0.7460	2	
	1.7452	1.5225	1.2460	1.0640	0.9166	0.8312	0.7751	0.7450	2	
	1.7399	1.5214	1.2427	1.0628	0.9205	0.8246	0.7746	0.7432	2	
	1.7445	1.5204	1.2416	1.0585	0.9212	0.8333	0.7817	0.7465	2	
	1.7420	1.5231	1.2244	1.0489	0.9171	0.8292	0.7828	0.7456	2	
Outer ring fault	1.7591	1.5345	1.2750	1.0757	0.9408	0.8476	0.7889	0.7547	3	
	1.7595	1.5363	1.2797	1.0834	0.9359	0.8467	0.7812	0.7458	3	
	1.7584	1.5395	1.2952	1.0955	0.9455	0.8473	0.7917	0.7558	3	
	1.7570	1.5317	1.2817	1.088	0.9417	0.8512	0.7844	0.7435	3	
	1.7553	1.5397	1.2876	1.0848	0.9312	0.8485	0.7851	0.7459	3	
Rolling element fault	1.7593	1.5353	1.3019	1.0900	0.9386	0.8447	0.7747	0.7425	4	
	1.7613	1.5305	1.2670	1.0756	0.9340	0.8305	0.7685	0.7371	4	
	1.7557	1.5218	1.2828	1.0797	0.9286	0.8324	0.7781	0.7429	4	
	1.7592	1.5325	1.2767	1.0711	0.9275	0.8257	0.7714	0.7330	4	
	1.7602	1.5365	1.2765	1.0731	0.9246	0.8213	0.7672	0.7334	4	

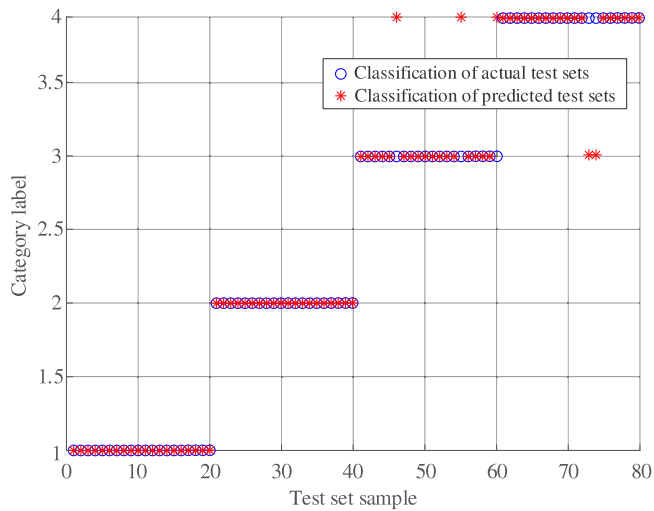


Fig. 15. Diagnostic results obtained using ICEEMDAN algorithm.

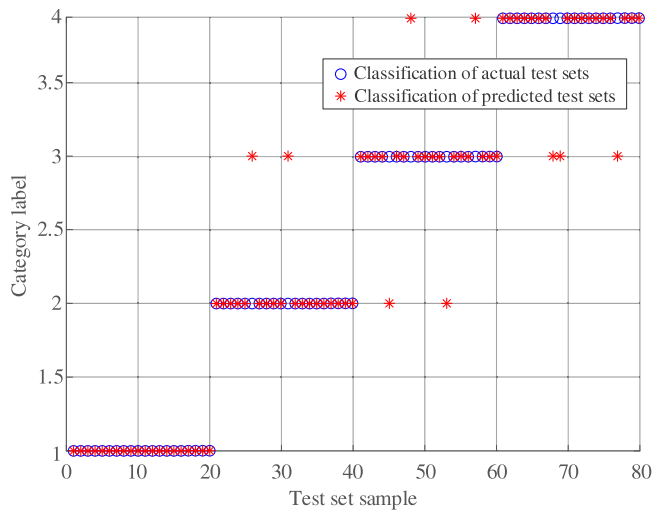


Fig. 16. Diagnostic results obtained using EEMD algorithm.

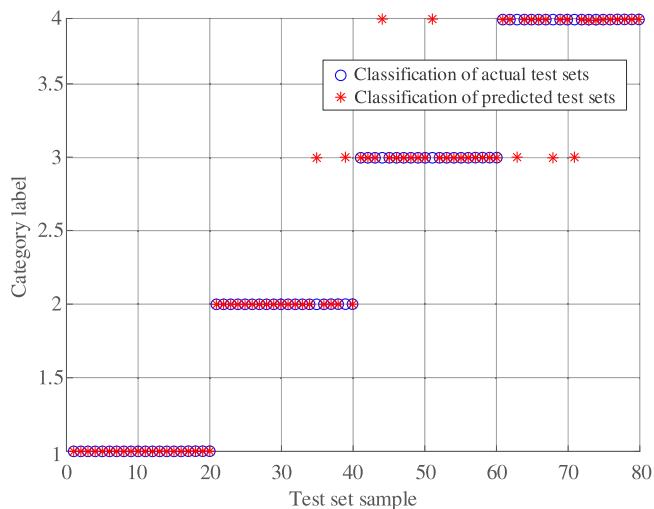


Fig. 17. Diagnostic results obtained using CEEMDAN algorithm.

Table 4

Classification accuracy of the four algorithms.

Algorithm	The correct rate of each time					Average correct rate
EEMD	88.75	86.25	87.5	87.5	88.75	87.75
CEEMDAN	91.25	92.5	92.5	90	91.25	91.5
ICEEMDAN	93.75	93.75	92.5	93.75	92.5	93.1
Methods of this paper	100	100	97.5	100	100	99.5

which masks the characteristics of the signal, so that the fault diagnosis rate decreases.

In order to further verify the diagnostic accuracy of each model, the signals are input into EEMD and CEEMDAN models for decomposition and fault classification. From the classification results, the diagnostic rates of the test data of EEMD and CEEMDAN models are 88.75% and 91.25% respectively (see Figs. 16 and 17).

To avoid the error in a single test, four more tests are conducted following the above steps, and the test results, i.e., the classification accuracy rate, are shown in Table 4. As can be seen from the table, The classification accuracy of EEMD and CEEMDAN is 87.75% and 91.5%, and the overall classification accuracy is low, indicating that the effect of fault feature extraction is poor. The accuracy of the improved self-selected ICEEMDAN algorithm is much higher than that of the unmodified ICEEMDAN algorithm, and the accuracy of fault diagnosis is increased by 6.4%, which shows that the algorithm proposed in this paper has certain advantages in bearing feature extraction.

6. Conclusions

Through analyzing and simulating, the verification of measured signals as well as testing the measured signal of the testbed, the improved self-selected ICEEMDAN algorithm proposed in this paper has excellent decomposition performance, and the new feature extraction of rolling bearings can be realized by combining with the permutation entropy algorithm. The conclusions are as follows:

1. Through the simulation signal analysis, compared with the traditional empirical mode decomposition algorithm, the improved self-selected ICEEMDAN algorithm has an excellent decomposition effect and the ability to suppress modal aliasing.
2. The bearing dataset of Case Western Reserve University is used for verification, and the energy entropy obtained by the improved self-selected ICEEMDAN and permutation entropy algorithm can effectively separate the vibration signal characteristics of bearings in different states, which can be used to characterize the characteristics of different bearing signals.
3. Through the test of the measured signals on the testbed, it is found that the improved self-selected ICEEMDAN algorithm has excellent performance, and it can be combined with permutation entropy algorithm and PSO-SVM algorithm to realize the fault diagnosis of rolling bearings, with the diagnosis accuracy rate of 99.5% and excellent diagnosis effect. Under the condition of keeping other algorithms unchanged, the improved self-selected ICEEMDAN algorithm improves the fault diagnosis accuracy by 6.4% compared with the common ICEEMDAN algorithm, and the diagnosis effect is more excellent.

Declaration of competing interest

The authors declare that they have no known competing financial interests or personal relationships that could have appeared to influence the work reported in this paper.

Acknowledgments

The research is funded partially by the Jiangsu International Science and Technology Cooperation Project, China (BZ2022002), the Jiangsu Province Agricultural Science and Technology Independent Innovation, China Project (CX(22)3101) and the National key research and development program, China (2022YFD2001805).

References

- [1] Xu J, Huang J, Zhao Y, et al. A robust intelligent fault diagnosis method for rolling bearings based on deep convolutional neural network and domain adaptation. *Procedia Comput Sci* 2020;174:400–5.
- [2] Gu R, Chen J, Hong R, et al. Incipient fault diagnosis of rolling bearings based on adaptive variational mode decomposition and teager energy operator. *Measurement* 2020;149:106941.
- [3] Wu J, Wu C, Cao S, et al. Degradation data-driven time-to failure prognostics approach for rolling element bearings in electrical machines. *IEEE Trans Ind Electron* 2019;66(1):529–39.
- [4] Feng Li, Tang T, Tang B, et al. Deep convolution domain-adversarial transfer learning for fault diagnosis of rolling bearings. *Measurement* 2020;169(5):108339.
- [5] Yuan S, Wang H, Sun X. Research on intermittent fault diagnosis of rolling bearings based on interval-valued evidence construction and possibility. *Measurement* 2022;203:111958.
- [6] Sun Y, Wang J, Wang X. Fault diagnosis of mechanical equipment in high energy consumption industries in China: A review. *Mech Syst Signal Process* 2023;186: 109833.
- [7] Suryawanshi Ganesh L, Patil Sachin K, Desavale Ramchandra G. Dynamic model to predict vibration characteristics of rolling element bearings with inclined surface fault. *Measurement* 2021;184(1):109879.
- [8] Kumar Anil, Gandhi CP, Zhou YQ, et al. Fault diagnosis of rolling element bearing based on symmetric cross entropy of neutrosophic sets. *Measurement* 2020;152: 107318.
- [9] Mishra C, Samantaray AK, Chakraborty G. Rolling element bearing fault diagnosis under slow speed operation using wavelet de-noising. *Measurement* 2017;103: 77–86.
- [10] Ni Q, Ji JC, Benjamin Halkon, et al. A fault information-guided variational mode decomposition (FIVMD) method for rolling element bearings diagnosis. *Mech Syst Signal Process* 2022;164(5):108216.
- [11] Zhao L, Zhang Y, Zhu D. Summary of research on fault diagnosis and prediction methods of rolling bearings in complex equipment. *China Test* 2020;46(3):17–25.
- [12] Prashant Kumar, Shankar Hati Ananda. Dilated convolutional neural network based model for bearing faults and broken rotor bar detection in squirrel cage induction motors. *Expert Syst Appl* 2022;191:116290.
- [13] Grover Chhaya, Turk Neelam. Rolling element bearing fault diagnosis using empirical mode decomposition and hjorth parameters. *Procedia Comput Sci* 2020; 167:1484–94.
- [14] Wang R, Jiang H, Zhu K, et al. A deep feature enhanced reinforcement learning method for rolling bearings fault diagnosis. *Adv Eng Inform* 2022;54:101750.
- [15] Ma C, Li Y, Wang X, et al. Early fault diagnosis of rotating machinery based on composite zoom permutation entropy. *Reliab Eng Syst Saf* 2023;230:108967.
- [16] Sun J, Liu Z, Wen J, et al. Multiple hierarchical compression for deep neural network toward intelligent bearing fault diagnosis. *Eng Appl Artif Intell* 2022;116: 105498.
- [17] Huang N, Shen Z, Long S, et al. The empirical mode decomposition and the Hilbert spectrum for nonlinear and non-stationary time series analysis. *Proc: Math Phys Eng Sci* 1998;454(1971):903–95.
- [18] Saidi Lotfi, Ali Jaouher Ben, Fnaiech Farhat. Bi-spectrum based-EMD applied to the non-stationary vibration signals for bearing faults diagnosis. *ISA Trans* 2014;53(5): 1650–60.
- [19] Liu X, Bo L, Luo H. Bearing faults diagnostics based on hybrid LS-SVM and EMD method. *Measurement* 2015;59:145–66.
- [20] Wang H, Chen J, Dong G. Feature extraction of rolling bearing's early weak fault based on EEMD and tunable Q-factor wavelet transform. *Mech Syst Signal Process* 2014;48:1–2.
- [21] Xue H, Ding D, Zhang Z, et al. A fuzzy system of operation safety assessment using multi-model linkage and multi-stage collaboration for in-wheel motor. *IEEE Trans Fuzzy Syst* 2022;30(4):999–1013.
- [22] Stazewski WJ, Tomlinson GR. Application of the wavelet transform to fault detection in a spur gear. *Mech Syst Signal Process* 1994;8(3):289–307.
- [23] Zhu X, Wang F, Li S. Harmonic detection method based on the improved ensemble empirical mode decomposition. *J New Ind* 2019;9(1):8–12.
- [24] Xue H, Wu M, Zhang Z, et al. Intelligent diagnosis of mechanical faults of in-wheel motor based on improved artificial hydrocarbon networks. *ISA Trans* 2022;120: 360–71.
- [25] Yang L, Hu Q, Zhang S. Research on fault feature extraction method of rolling bearings based on the improved wavelet threshold and CEEMD. *J Phys Conf Ser* 2020;1449:012003.
- [26] Chen J, Fu H, Wang Y, et al. A fault diagnosis method for a practical engineering application based on CEEMD and ELM. *Vibroeng Procedia* 2017;11:46–51.
- [27] Wang J, Li Z, Wang D. A method for wavelet threshold denoising of seismic data based on CEEMD. *Geophys Prospect* 2014;53(2):164–72.
- [28] Torres M, Coliminas M, Schlotthauer G, et al. A complete ensemble empirical mode decomposition with adaptive noise. In: *IEEE international conference on acoustics, speech and signal processing*. 2011, p. 4144–7.
- [29] Li Y, Chen X, Yu J. A hybrid energy feature extraction approach for ship-radiated noise based on CEEMDAN combined with energy difference and energy entropy. *Processes* 2019;7(2):69.
- [30] Bai L, Han Z, Ren J, et al. Fault diagnosis method for rolling bearings based on CEEMDAN and permutation entropy. *Taiyuan Univ Technol* 2019;(11):54–9.
- [31] Liu Z, Lv K, Zheng C, et al. A fault diagnosis method for rolling element bearings based on ICEEMDAN and Bayesian network. *J Mech Sci Technol* 2022;36(5):1–12.
- [32] Zhang P, Li Y, Liu W. Research on bearing fault diagnosis based on ICEEMDAN and SVM. *Technol Mark* 2022;29(07):103–5.
- [33] Feng Y, Gao J. Bearing fault diagnosis based on ICEEMDAN energy moment and MFOA-PNN. *Modern Manuf Eng* 2022;(03):122–126+153.
- [34] Wang G, Zhang M, Hu Z, et al. Bearing fault diagnosis based on multi-scale mean permutation entropy and parameter optimization support vector machine. *Vib Shock* 2022;41(1):221–8.
- [35] Feng F, Rao G, Si A, et al. Application and development of permutation entropy algorithm. *J Armored Forces Eng College* 2012;26(2):34–8.
- [36] Zhao Q, Chen F, Gan L, et al. Short term wind power prediction based on EEMD-PSO-svm. *Modern Electron Technol* 2021;44(15):89–93.
- [37] Zhang L, Xiao J. *Case course of mechanical fault diagnosis technology based on MATLAB*. Beijing: Higher Education Press; 2016.
- [38] Xiao M, Zhang C, Fu X, et al. Fault feature extraction method of rolling bearings based on ICEEMDAN and wavelet threshold. *J Nanjing Agric Univ* 2018;41(4): 767–74.
- [39] Hu C, Li A. Detection and extraction method of EMD intermittent signal. *Data Acquis Process* 2008;(1):108–11.
- [40] Kizhner S, Flatley T, Huang N. On the Hilbert-huang transform data processing system development. In: *IEEE aerospace conference proceedings*. USA: Big Sky Montana; 2004. p. 1961–79.